Electronic Supplementary Material (ESI) for Journal of Materials Chemistry A.

***In-situ* Textured Carbon Nitride Photoanodes with Enhanced Photoelectrochemical Activity by Band-Gap State Modulation:** *in-situ* texture of oxygen-doped carbon nitride film was prepared by MSTVC method, realizing enhanced light absorption and charge separation simultaneously. The remarkable PEC performance addresses the importance of nanoengineering from composition regulation and morphology control.

Keyword

M. Huang, H. Wang, Wan Li, Y.-L. Zhao* and R.-Q. Zhang*

***In-situ* Textured Carbon Nitride Photoanodes with Enhanced Photoelectrochemical Activity by Band-Gap State Modulation**

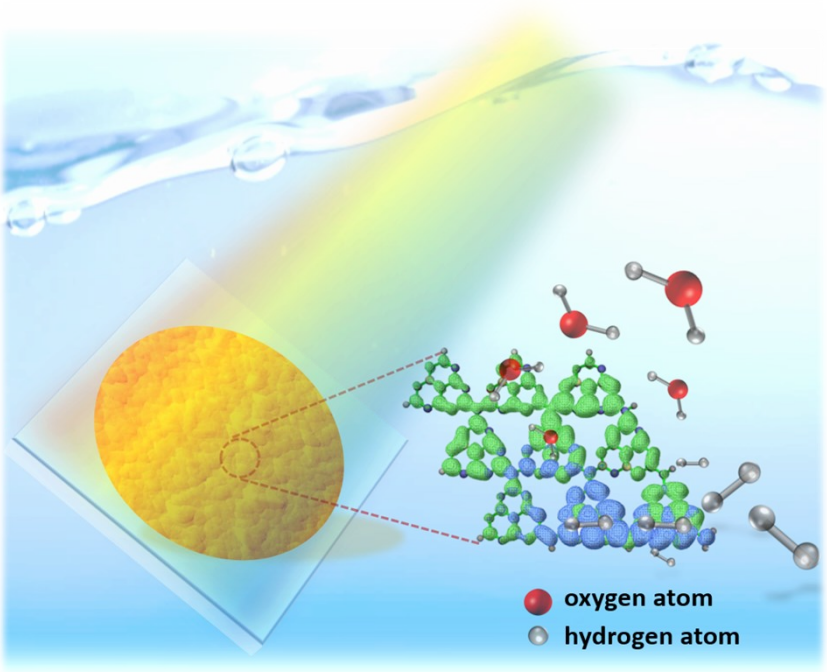

Supporting Information

In-situ Textured Carbon Nitride Photoanodes with Enhanced Photoelectrochemical Activity by Band-Gap State Modulation

*Miaoyan Huang,[a,b] Haipeng Wang,[a] Wan Li,[c] Yan-Ling Zhao,[*a,d] and Rui-Qin Zhang[*a,b]*

M. Huang, H. Wang, W. Li, Y.-L. Zhao, R.-Q. Zhang
City University of Hong Kong
83 Tat Chee Avenue, Hong Kong SAR 999077, China
E-mail: aprqz@cityu.edu.hk; apzyl@cityu.edu.hk

M. Huang, R-Q. Zhang
Shenzhen JL Computational Science and Applied Research Institute
Shenzhen, China

W. Li
Institute of Research & Development, Centre Testing International Group Co.
Shenzhen China.

Y.-L. Zhao
Shenzhen Research Institute, City University of Hong Kong, Shenzhen 518057, China

One-step thermal vapor condensation (TVC): In a typical TVC routine, a piece of FTO glass was evenly placed on the top of a finely polished crucible (25 mL) with 10 g of melamine inside. They were transferred to a muffle furnace and heated to 600 ºC with a constant heating rate of 3 ºC/min.

Multistep thermal vapor condensation (MSTVC): The optimized MSTVC method is described in the Experimental Section. The heating rates applied in other kinds of MSTVC methods are listed in Table S1:

Table S1. The heating rates applied in different temperature intervals

Method	300-390 °C (°C/min)	390-520 °C (°C/min)	520-600 °C (°C/min)
MSTVC	1.5	3	3
MSTVC-a	1.5	10	3
MSTVC-b	10	10	3
MSTVC-c	N/A	N/A	3[a)]

[a)]The setup was transferred directly to the muffle without the previous two steps.

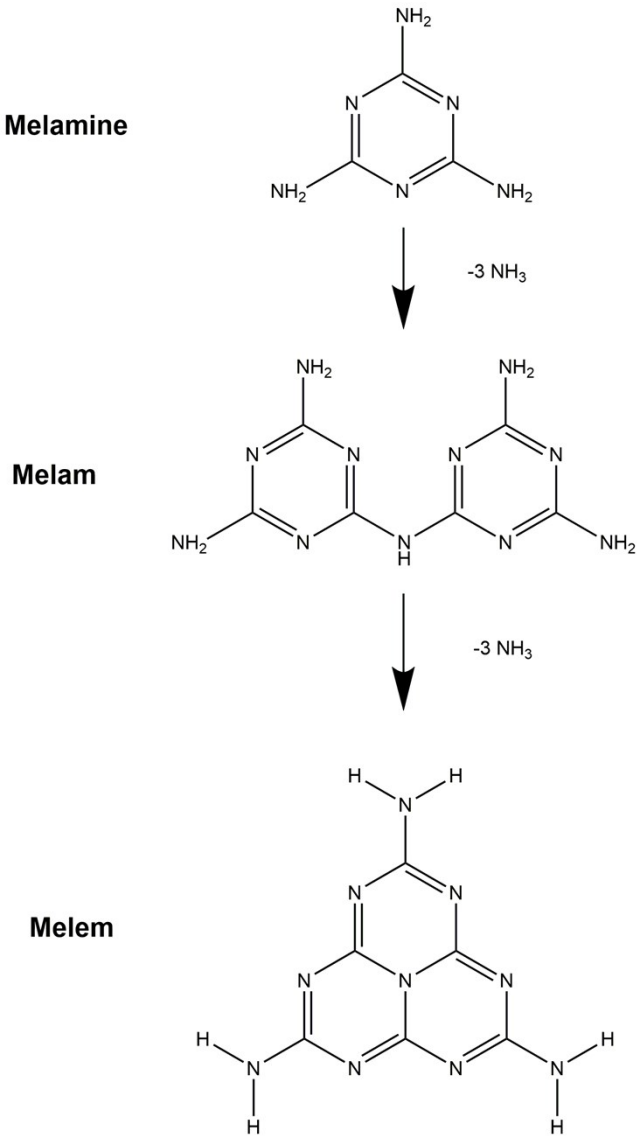

Figure S1. Reaction path for the formation of melem starting from melamine.

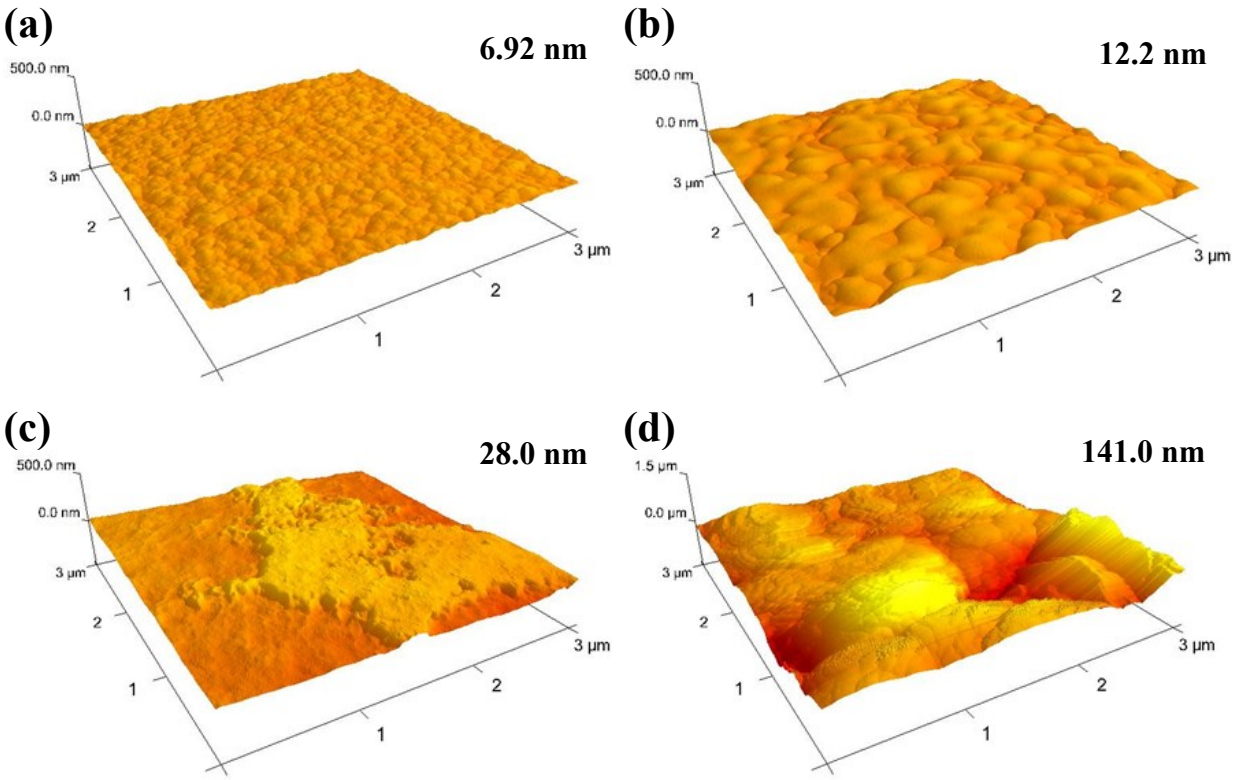

Figure S2. (a) Pristine CN film prepared by the MSTVC method, (b) prepared by the MSTVC-a method, (c) prepared by the MSTVC-b method and (d) prepared by the MSTVC-c method.

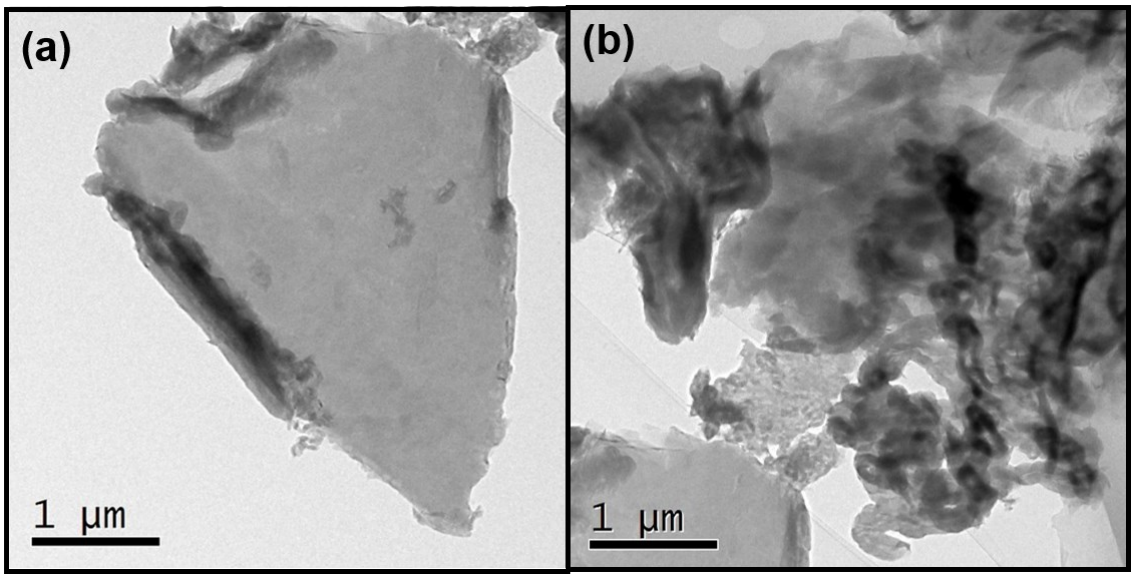

Figure S3. TEM images of (a) SCN film and (b) CN film.

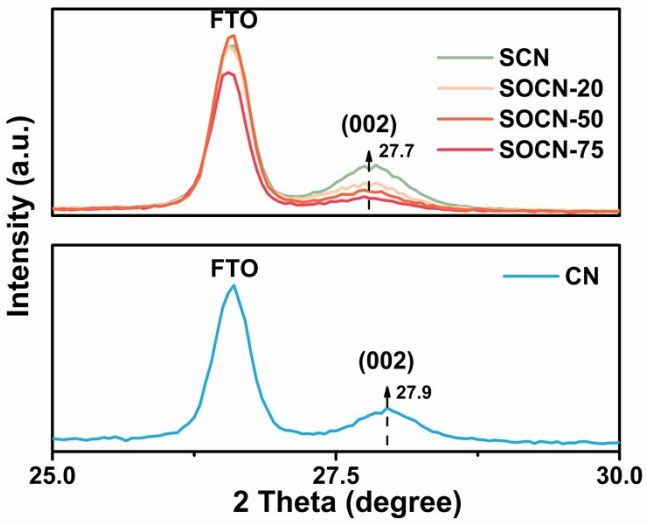

Figure S4. XRD patterns of CN, SCN, SOCN-20, SOCN-50 and SOCN-75 films.

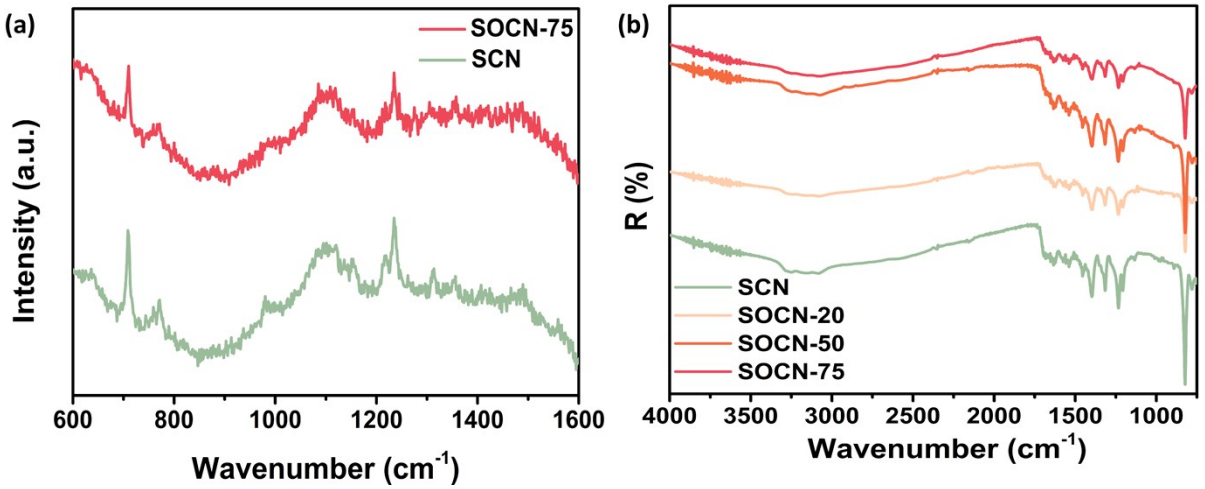

Figure S5. (a) Raman spectra of SCN and SOCN-75 recorded with a 532 nm laser as the excitation source. The Raman peaks appearing at about 710 and 990 cm^{-1} are attributed to different types of ring breathing modes for triazines or heptazines in g-CN. SOCN-75 films show the same Raman pattern with pristine films but at lower intensity. The signal was stretched and low intensity because of the relatively low film thickness. (b) FTIR spectra of different films.

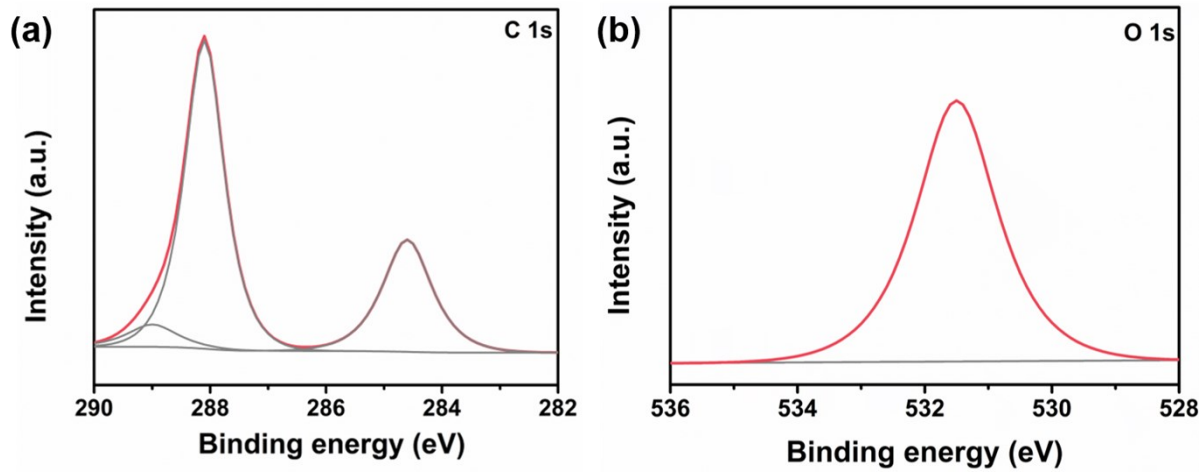

Figure S6. The high-resolution (a) C 1s and (b) O 1s spectra of SOCN-75 film after Ar^+ etching.

Table S2. Surface composition obtained by XPS after Ar^+ etching

Film	**C (at. %)**	**N (at. %)**	**O (at. %)**
SCN	56.4	43.6	trace amount
SOCN-20	56.1	42.8	1.1
SOCN-50	55.0	42.7	2.3
SOCN-75	54.2	41.1	4.7

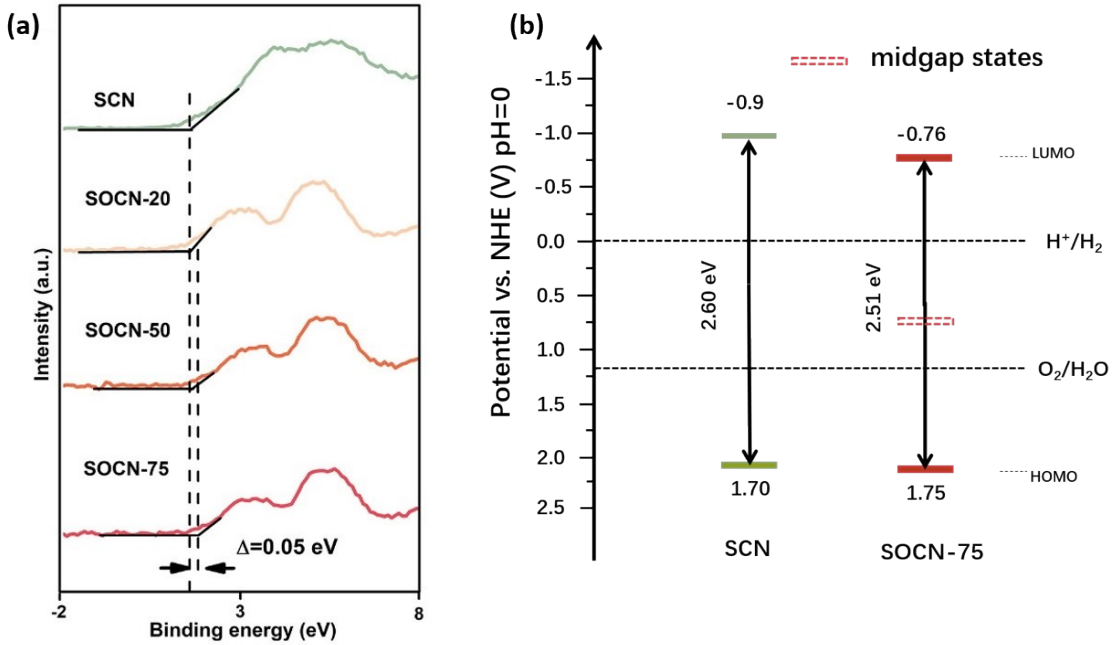

Figure S7. (a) XPS valence band position. (b) Schematic illustration of SCN and SOCN-75 film band structure.

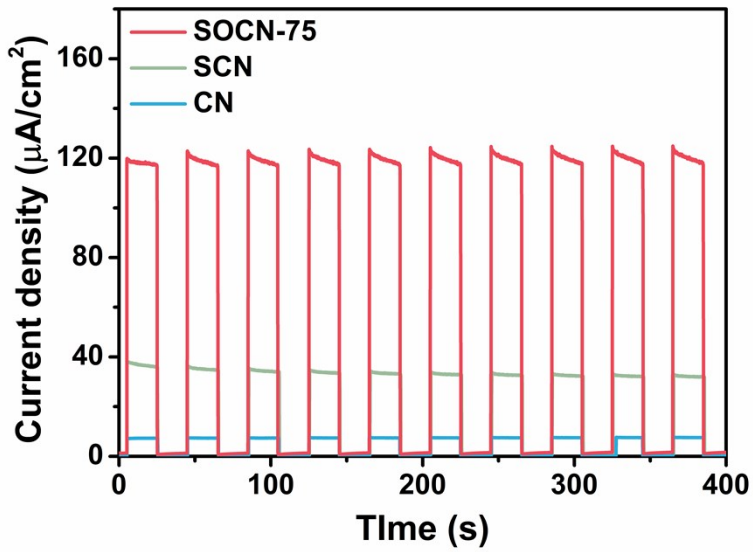

Figure S8. The transient photocurrent density curves of different CN films with a duration of 400 s and a chop interval of 20 s. Electrolyte: 0.2 M Na_2SO_4.

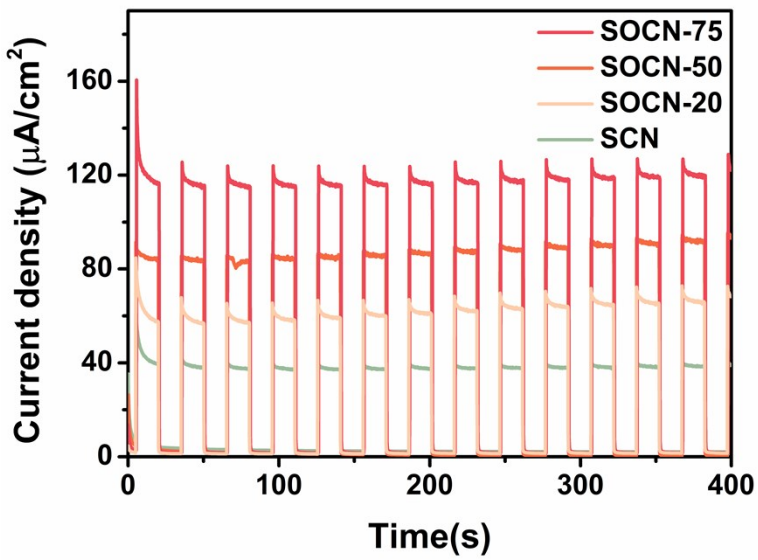

Figure S9. The transient photocurrent density curves of different SOCN-*x* films with a duration of 400 s and a chop interval of 15 s. Electrolyte: 0.2 M Na_2SO_4.

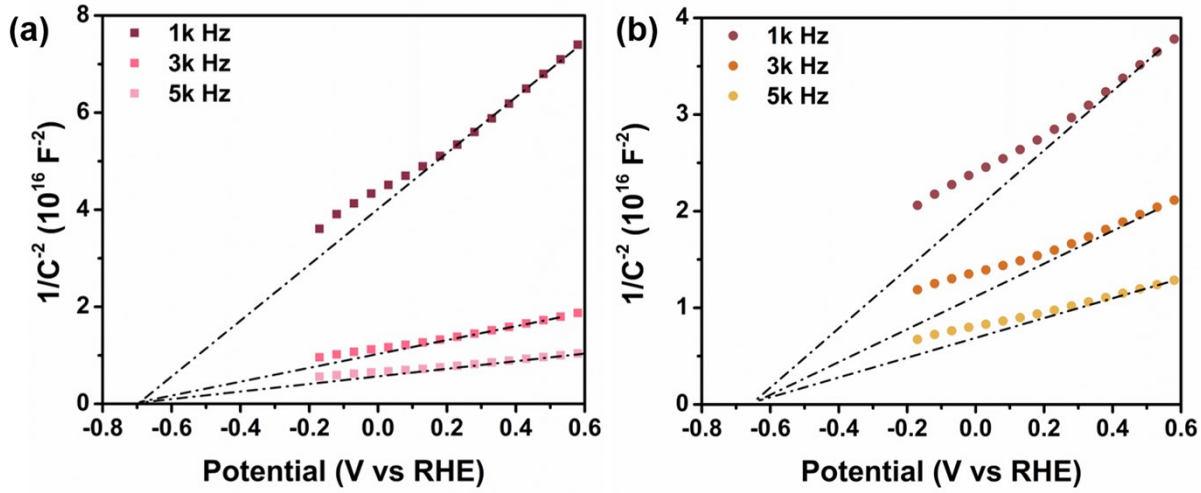

Figure S10. Mott-Schottky plots of (a) SCN and (b) SOCN-75 film with sinusoidal modulation at the frequencies of 1000, 3000, and 5000 Hz, respectively.

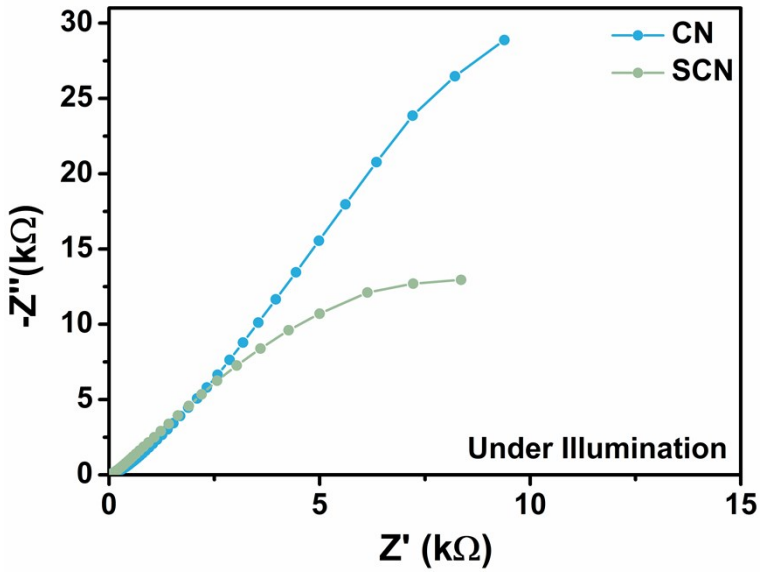

Figure S11. The Nyquist plots under illumination.

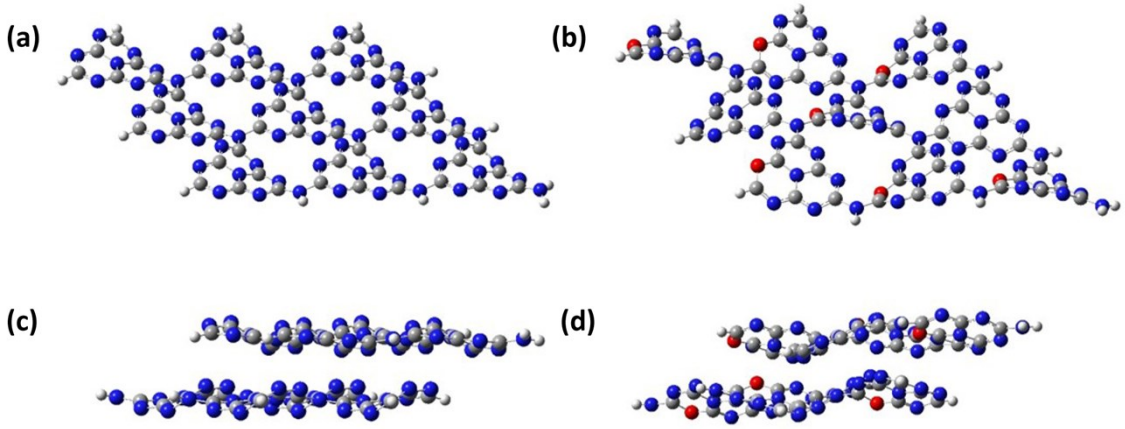

Figure S12. Top views of one-layer (a) CN and (b) OCN films with seven bay-site N substituted by O atoms. Side views of two-layer (c) CN and (d) OCN films with seven bay-site N substituted by O atoms.

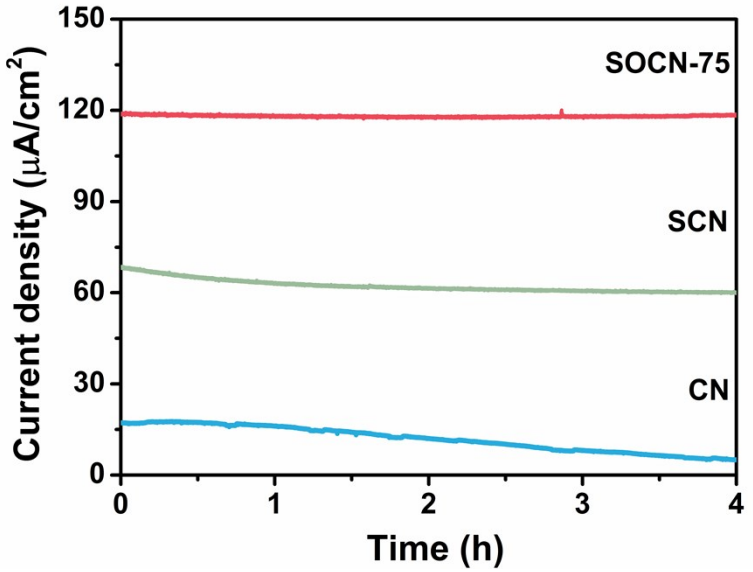

Figure S13. Stability test of CN, SCN and SOCN-75 films under 1 sun illumination for 4 h. Electrolyte: 0.2 M Na_2SO_4 and 0.05 M Na_2S.

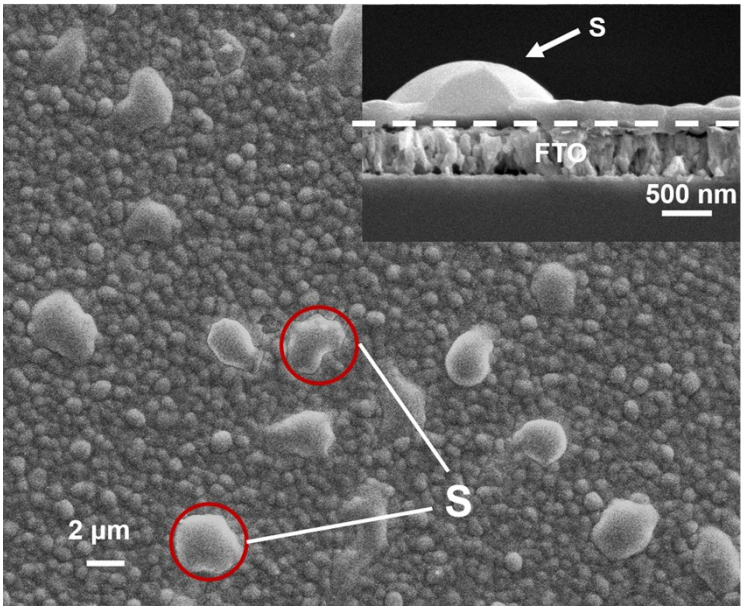

Figure S14. Top-view and cross-sectional SEM images (inset) of the SOCN-75 film after 4 h stability evaluation.

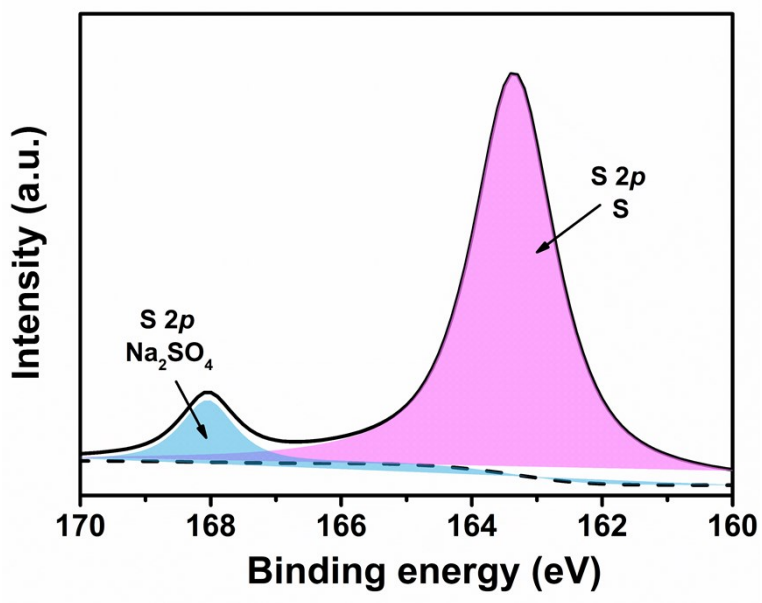

Figure S15. High resolution XPS spectra of S.

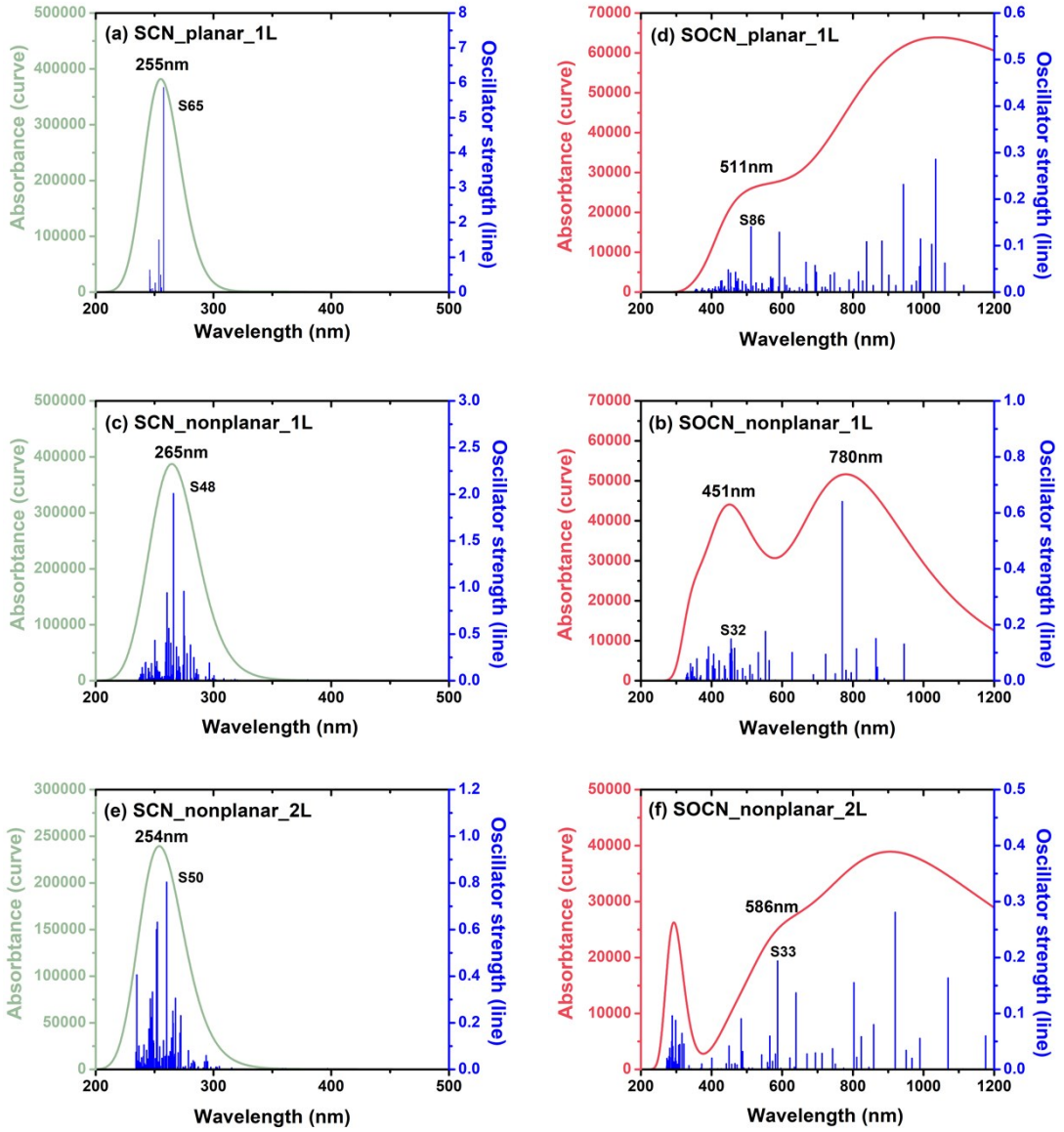

Figure S16. UV-vis absorption spectra of pristine carbon nitride and oxygen doped carbon nitride that adopting different structures based on TD-DFT calculations (TD-ωB97XD/6-31G*)

Table S3. Summary of PEC water oxidation performance of CN based photoanodes

Film	**Photocurrent density** ($\mu A\ cm^{-2}$)	**Potential** (V vs. RHE)	**ref**
CN film	30.2	1.23	[1]
CN/rGO/NiFe-layered double hydroxide	72.9	1.22	[2]
CN film	70	1.23	[3]
CN film	63	1.23	[4]
3%Ni-CN	69.8	1.23	[5]
CN porous film	12	1.23	[6]
Nanojunction CN film	103.2	1.23	[7]
g-CN nanorod array	10.8	1.23	[8]
Boron-doped CN	45	1.23	[9]
CN-rGO0.5	75	1.23	[10]
CN film	89	1.1	[11]
SOCN-75	119.2	1.23	Our work

References

[1] J. Liu, H. Wang, Z. P. Chen, H. Moehwald, S. Fiechter, R. van de Krol, L. Wen, L. Jiang, M. Antonietti, *Adv. Mater*. **2015,** *27*, 712.

[2] Y. Hou, Z. Wen, S. Cui, X. Feng, J. Chen, *Nano lett.* **2016,** *16*, 2268.

[3] J. Bian, L. Xi, C. Huang, K. M. Lange, R. Q. Zhang, M. Shalom, *Adv. Energy Mater.* **2016,** *6*, 1600263.

[4] X. Lv, M. Cao, W. Shi, M. Wang, Y. Shen, *Carbon* **2017,** *117*, 343.

[5] W. Zhang, J. Albero, L. Xi, K. M. Lange, H. Garcia, X. Wang, M. Shalom, *ACS Appl. Mater. Interfaces* **2017,** *9*, 32667.

[6] G. Peng, L. Xing, J. Barrio, M. Volokh, M. Shalom, *Angew. Chem. Int. Ed*. **2018,** *130*, 1200.

[7] Q. Ruan, W. Luo, J. Xie, Y. Wang, X. Liu, Z. Bai, C. J. Carmalt, J. Tang, *Angew. Chem. Int. Ed.* **2018,** *56*, 8221.

[8] R. Wang, H. Liu, Z. Fan, L. Li, Y. Cai, G. Xu, W. Luo, B. Yang, Y. Zhou, Z. Zou *Nanoscale* **2018,** *10*, 3342.

[9] M. Huang, Y. L. Zhao, W. Xiong, S. V Kershaw, Y. Yu, W. Li, T. Dudka, R. Q. Zhang, *Appl. Catal. B Environ*. **2018,** *237*, 783.

[10] G. Peng, M. Volokh, J. Tzadikov, J. Sun, M. Shalom, *Adv. Energy Mater.* **2018**, 1800566.

[11] X. Lu, Z. Liu, J. Li, J. Zhang, Z. Guo, *Appl. Catal. B Environ*. **2017**, 209, 657.